Carbon-13 NMR relaxation studies of pre-melt structural dynamics in [4-^{13}C-uracil] labeled *E. coli* transfer RNA$_1^{Val}$*

Jay I.Olsen[1], Martin P.Schweizer[1,3], Irene J.Walkiw[1,4], W.David Hamill, Jr.[2,5], W.James Horton[2] and David M.Grant[2]

Departments of [1]Medicinal Chemistry and [2]Chemistry, University of Utah, Salt Lake City, UT 84112, USA

Received 6 April 1982; Revised and Accepted 21 June 1982

ABSTRACT

We report 67.8 MHz carbon-13 spin-lattice relaxation studies on [4-^{13}C-uracil] labeled tRNA$_1^{Val}$ purified from E. coli SO-187. Following ^{13}C-enriched C_4 carbonyl resonances from modified and unsubstituted uridines scattered throughout the polymer backbone enables us to determine dynamical features in both loop and helical stem regions. The experimental results have been analyzed in terms of a model of isotropic overall molecular reorientation. "Anomalous" residues for which the experimental data cannot be accounted for in terms of the model provide an assessment of local and regional properties. Thus, "native" tRNA$_1^{Val}$ under physiological conditions of magnesium (10 mM) and temperature (20°-40°C), exhibits the following characteristics: 1) uridines held rigidly in helical stems and tertiary interactions display correlation times for rotational reorientation of 15-20 nsecs, typical for overall tRNA motion; 2) uridines in loops such as the wobble residue uridine-5-oxyacetic acid (V_{34}) are quite accessible to solvent; moreover V_{34} and another loop residue, D_{17}, exhibit local mobility; 3) the tertiary interactions involving 4-thio uridine (s^4U_8) and A_{14} and ribothymidine (rT_{54}) and A_{58} are weakened as temperature increases.

INTRODUCTION

Nuclear magnetic resonance techniques applied to transfer RNA structure, conformation and interaction in solution have been utilized very extensively and fruitfully during the past few years, as evidenced by the yearly reviews on the subject (1-6). A large fraction of the studies on individual tRNA's have dealt with the low field imino and amino protons involved in hydrogen bonding and the non-exchangeable high field protons from assorted modified nucleosides usually located in loop segments. Other investigations utilizing natural abundance ^{31}P (7,8) and ^{13}C-nmr on specifically enriched residues (9-11) have appeared. Despite the considerable effort in obtaining site specifically ^{13}C-enriched individual tRNA's, the use of ^{13}C-nmr offers certain advantages: 1) wide chemical shift range; 2) ease of resonance assignment; and 3) ability to relate relaxation data to dynamic features of tRNA itself and in complexes with proteins of interest.

© IRL Press Limited, Oxford, England.

0305-1048/82/1014-4449$2.00/0

In the case of E. coli $tRNA_I^{Val}$, Reid and co-workers (4, 6, 12) have shown that the low field imino proton spectrum can be interpreted in terms of a folded structure with ∿ 7 tertiary hydrogen bond interactions and ∿ 20 secondary base-pairs, two of the latter shown by Johnston and Redfield (13) to be due to the G_{50}-U_{64} wobble base pair (Fig. 1). Solution structures of Class I tRNA's such as $tRNA_I^{Val}$ and $tRNA^{Phe}$ probably are fairly close to the crystal structure (14) determined for $tRNA^{Phe}$ (15,16), shown in Fig. 3.

In the presence of 10 mM magnesium ion,the E. coli $tRNA_I^{Val}$ solution structure as depicted in Fig. 3 is maintained to 45-50°C (12) at which point the tertiary interactions begin to be disrupted. We have an interest in the dynamics of the native structure of $tRNA_I^{Val}$ at physiologically relevant temperatures around 30-40°C and how this structure might be altered in the presence of cognate aminoacyl synthetase. In this paper we describe 67.8 MHz ^{13}C-spin-lattice relaxation and NOE investigations on [4-^{13}C-uracil] labeled $tRNA_I^{Val}$ of E. coli SO-187 as a function of temperature. We have monitored C_4 carbonyl resonances from eleven of the fourteen modified and unmodified uracil residues scattered throughout the loop and stem regions of this molecule (Fig. 1). Based upon a model of isotropic rotational reorientation, we have calculated motional correlation times at each of these residues. Residues which display anomalous behavior provide insights about local and regional dynamics. In addition, we have estimated the relative importance of chemical shift anisotropic (CSA), proton dipolar and nitrogen dipolar mechanisms to the spin-lattice relaxation processes.

METHODS

Isolation and purification of [4-^{13}C-uracil] labeled $tRNA_I^{Val}$ from the E. coli uracil auxotroph SO-187 was accomplished essentially as outlined earlier (9), except that homogeneous $tRNA_I^{Val}$ could be obtained in two chromatographic steps: 1) BD cellulose (ambient temperature) and 2) Sepharose 4B at 4°C using reverse $(NH_4)_2SO_4$ gradients. 19 mg of the $tRNA_I^{Val}$ was dissolved in a 0.4 ml solution of double deionized charcoal filtered water containing 20% D_2O (Stohler, 99.8% d), K_2HPO_4 (20 mM; pD 7.2), NaCl (50 mM), $MgCl_2$ (10 mM), EDTA (5 mM), $Na_2S_2O_3$ (3 mM), and 0.02% (w/v) NaN_3 to retard bacterial growth. The sample was placed in a 5 mm tube previously cleaned with 50% nitric acid. Even though dissolved oxygen would probably be a minor influence on the relaxation rate in the 0.2 - 0.5 sec^{-1} range found in this study, the $tRNA_I^{Val}$ sample was not degassed.

Carbon-13 NMR measurements at 67.8 MHz were conducted on a JEOL FX-270,

using proton noise decoupling at 2 watts power to prevent dielectric heating in these aqueous salt solutions. For these carbonyls we used a spectral window of 3 KHz, centered at 177 ppm from TMS. T_1 values were determined using the fast inversion-recovery method (17) with the sequence -(180°- τ - 90°(FID)-WT)n, where τ_∞ equals $5T_1$ (20 sec), waiting time, WT, between pulse trains equals $3T_1$ (12 sec) and n is 2000. Usually spectra were collected using 9 different τ values. Using the manufacturer's software, standard least squares fitting of the line intensities, A_i, at τ_i was conducted and T_1 values determined from the equation $\ln(A_\infty - A_i)/2A_0 = - _i/T_1$ where A_∞ is the limiting intensity at $\tau = 5T_1$ and A_0 is the extrapolated value for $\tau_i = 0$.

Nuclear Overhauser enhancements, η, were determined by comparing peak intensities in spectra taken with the decoupler on continuously and the decoupler gated off during a $5T_1$ delay between 90° observe pulses. Probe temperatures were controlled with a programmed variable temperature unit, previously calibrated with 1,3-propanediol.

RESULTS AND DISCUSSION

Based upon nmr studies of the imino and amino protons involved in secondary and tertiary hydrogen bonding interactions in *E. coli* $tRNA_I^{Val}$ (12), one may confidently assume that the general overall three-dimensional "native" structure of the molecule in solvent mileau containing 10 mM $MgCl_2$ is maintained over the 20-40°C temperature range under consideration here. Therefore the observed changes in relaxation parameters with temperature described below undoubtedly reflect segmental modulations of this basic molecular framework.

In Fig. 1 we display the primary sequence of *E. coli* $tRNA_I^{Val}$ [18, 19] arranged in the usual cloverleaf pattern with the [4-^{13}C] uridines underlined and the corresponding structures of these nucleosides as shown.

The 67.8 MHz carbon-13 spectra for [4-^{13}C-uracil]$tRNA_I^{Val}$ at the temperature extremes for this study, 20 and 40°C are presented in Fig. 2. These are the fully recovered "τ_∞ spectra" of the inversion-recovery measurements, where τ_∞ = 20 sec and 2000 transients were transformed. In addition to the four assigned resonances (assignment criteria were reported earlier (9) for S^4U_8, D_{17}, and V_{34}] T_{54} has subsequently been assigned via specific $^{13}C\{^1H\}$ decoupling) we have monitored unassigned resonances #3, 4, 5, 6, 7, 9 and 12 in the T_1 and NOE experiments.

Temperature increase generally results in line narrowing and shifts to lower field (Fig. 2). Of particular interest is the sharpening of S^4U_8 and the larger downfield shift of the V_{34} resonance ($\sim$0.5 ppm). The former may

be a result of disruption of the tertiary S^4U_8 - A_{14} interaction (12; see Fig. 3) while the latter undoubtedly comes about from flexibility in the anticodon loop enabling destacking of V_{34} from purine neighbors particularly A_{35}; (see Ref. 9).

Spin-lattice Relaxation

Hamill, et.al., (20) have previously described relaxation studies on [4-

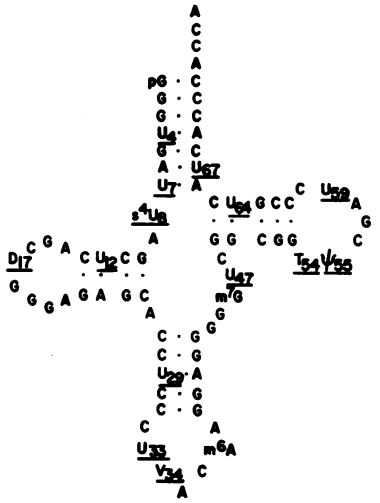

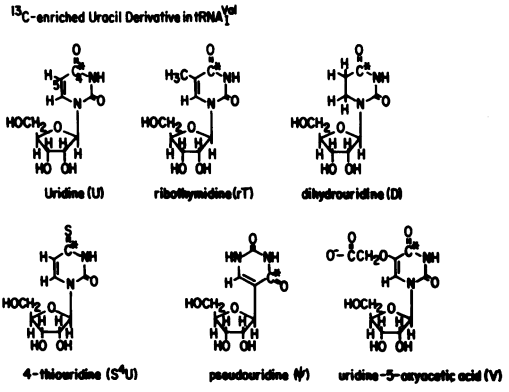

FIGURE 1. Top: cloverleaf representation of $tRNA_1^{val}$ sequence (18,19) with uridines having ^{13}C-enriched C_4 carbonyls underlined. The structures of these nucleosides are shown in the lower panel

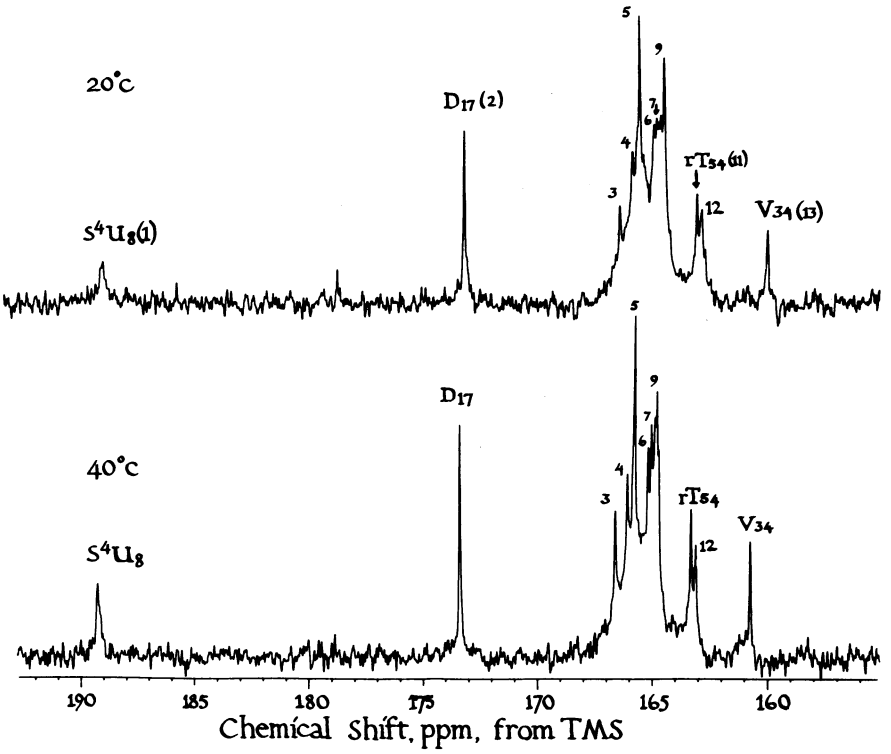

FIGURE 2. Fully recovered (τ_∞ = 20 sec.) spectra of 19 mg (4-^{13}C-ruacil) labeled $tRNA_1^{Val}$ in 0.4 ml 80/20 H_2O/D_2O system (see Methods). 2000 transients, 90° pulse width was 7.2 µsec.

^{13}C-uracil] labeled unfractionated tRNA of Salmonella typhimurium. In this work an assessment was made of the predominant relaxation mechanisms of the quaternary C_4 carbonyl carbon of the uracils as a function of magnetic field strength. The calculated contribution of chemical shift anisotropy to the spin-lattice relaxation increased from about 25% at 23.5 kG to about 80% at 84.6 kG, with less than 5-10% ^{14}N dipolar contribution and the remainder due to proton dipolar mechanisms. Experimentally the relaxation rate was found to decrease with increase in magnetic field although not as drastically as theory would predict for a molecule such as tRNA tumbling outside the extreme narrowing limit.

R_1 values obtained at 23.5 kG by Hamill, et. al, for S^4U, D and several uridines in the S. typhimurium mixture, at 37°C, in water are respectively 0.7, 0.59 and 0.59 to 0.67 sec^{-1}. From Figs. 4 and 5, the values we obtained

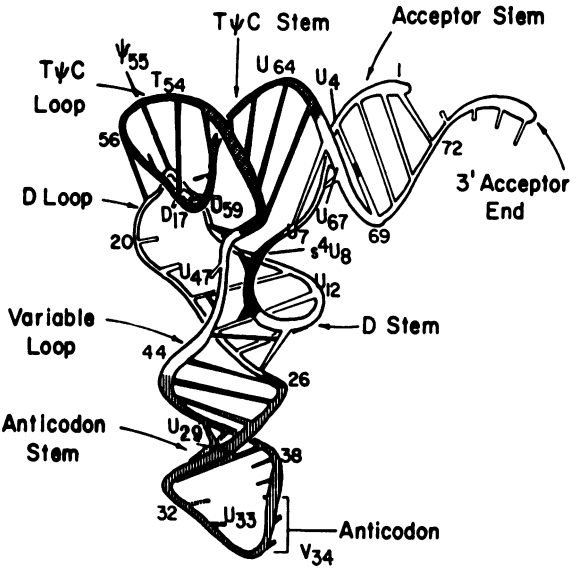

FIGURE 3. Three dimensional framework as per X-ray structure of yeast $tRNA^{phe}$ (15,16) with superimposed ^{13}C-enriched uridines as in E. coli $tRNA_1^{val}$.

at 63.5 kG, 34°C in 80/20 H_2O/D_2O are 0.47, 0.34 and 0.3 to 0.4 sec^{-1}. These significantly lowered values confirm that $tRNA_1^{val}$ is undergoing molecular reorientation with a correlation time, τ_R, to the right of the R_1 vs τ_R maximum, e.g. outside the extreme narrowing region.

Spin-lattice relaxation times at several temperatures for the uracil C_4 carbonyl resonances of [4-^{13}C-uracil] labeled $tRNA_1^{val}$ are presented in Table I. The corresponding relaxation rates, $R_1(sec^{-1})$, for the samples in 80/20 H_2O/D_2O solution are plotted in Figs. 4 and 5 versus temperature. From the different dependencies seen here, we designate three "classes" of uridines: Class I - large increases in R_1 vs. temperature, e.g., S^4U_8, #3, and #12 (Figs. 2 and 4); Class II - moderate increase in R_1 vs. temperature, e.g., #4, 5, 6, 7, 9 and rT_{54} (Fig. 2 and 5); Class III - very little net change in R_1, e.g., D_{17} and V_{34} (Figs. 2 and 5).

We consider that the uridines whose C_4 carbonyl resonances exhibit a small but consistent increase in R_1 vs. temperature are those which are located in helical H-bonded stems and H-bonded tertiary folding and thus experience molecular reorientation similar to that of the tRNA molecule itself. Since we know from the field effect on R_1 mentioned above that the

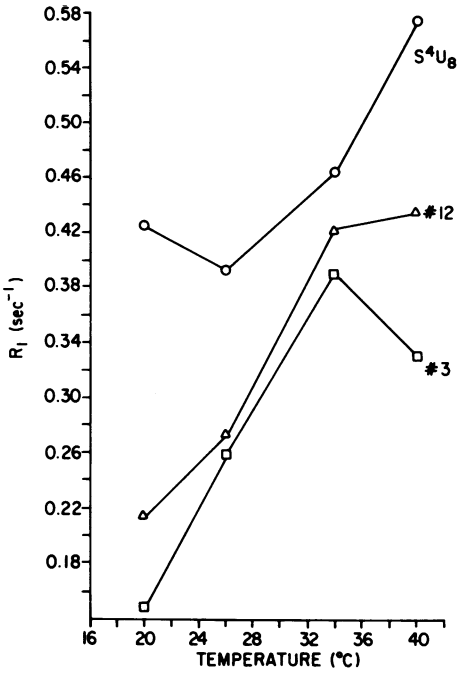

FIGURE 4. Spin lattice relaxation rates, R_1 (sec^{-1}) versus temperature for highly dependent uridines (Class I). Error estimate ± 0.02 sec^{-1}.

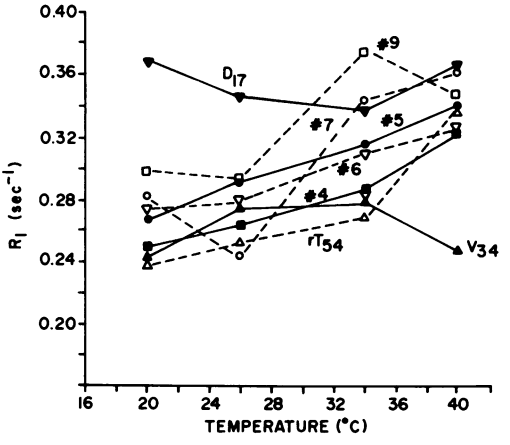

FIGURE 5. Spin lattice relaxation rates, R_1 (sec^{-1}) versus temperature for slightly dependent (Class II) and essentially independent (Class III) uridines. Error estimate ± 0.02 sec^{-1}.

TABLE I

SPIN LATTICE RELAXATION TIMES FOR URACIL C_4 CARBONYLS IN E. COLI $tRNA_I^{Val}$ (a)

PEAKS	ASSIGNMENT AND CHEMICALS SHIFTS	20° (b)	26°	34° (H_2O)	34° (D_2O)	40°
1	S^4U_8 (189.3)	2.34	2.54	2.15	2.86	1.74
2	D_{17}(173.4)	2.71	2.89	2.97	3.38	2.73
3	U (166.6)	6.65	3.85	2.55	4.86	2.03
4	U (166.1)	3.98	3.78	3.49	4.54	3.09
5	U (165.8)	3.72	3.43	3.17	3.77	2.94
6	U (165.2)	3.63	3.59	3.22	Overlapping	3.09
7	U (165.0)	3.55	4.12	2.92		2.77
8	U	c	c	c	c	2.34
9	U (164.7)	3.34	3.40	2.67	3.74	2.88
10	U	d	d	d	d	2.66
11	rT_{54}(163.3)	4.19	3.96	3.70	4.79	2.96
12	U (163.1)	4.62	3.64	2.37	4.94	2.30
13	V_{34}(160.4)	4.09	3.62	3.60	>8-9[e]	4.05

(a) Values are in seconds, measured at 67.8 MHz via fast inversion-recovery method. (Canet, et. al., 1975). 2000 transients transformed. Estimated error ± 10% or less.

(b) Chemical shifts measured from internal dioxane in another $tRNA_I^{Val}$ sample and converted to TMS by adding 66.3 ppm.
(c) Peak observed, but not processed in computer calculations.
(d) Peak not resolved
(e) This value may be underestimated since τ_∞ = 30 sec was used.

correlation time, τ_R, for overall reorientation of the tRNA lies to the right of the R_1 vs. τ_R maximum, it would be expected that as temperature increases and τ_R becomes smaller that R_1 should increase until the maximum is reached.

Calculated Relaxation Parameters

In order to estimate the correlation times for rotational reorientation of the various uridines and modified uridines and to assess the contributions of proton-dipolar, nitrogen-dipolar and chemical shift anisotropy mechanisms, we have utilized the following treatment. We assume an isotropic tumbling model and consider only auto correlated internuclear spin pairs in the dipole-dipole mechanism. We justify, in part, the neglect of cross-correlated interactions involving three or four nuclear spins on the basis that our data did not exhibit any pronounced deviations from single exponential behavior, and since initial slopes depend only on auto correlated terms there is insufficient information to characterize the importance of such terms. Finally, relaxation data on macromolecules such as tRNA unfortunately do not have

intrinsic accuracy sufficient to provide cross-correlation data in the inversion recovery type experiments on total carbon magnetization in the proton decoupled experiment. The following equations for isotropic tumbling were therefore used:

$$R = \frac{1}{T_1} = R_{CSA} + \sum_S R_{IS} \tag{1}$$

$$R_{CSA} = \frac{1}{T_{1CSA}(I)} = \frac{1}{15} (\gamma_C H_0)^2 \Delta\sigma^2 J(\omega_I) \tag{2}$$

$$R_{IS} = \frac{1}{T_1(IS)} = \frac{N_S \hbar^2 \gamma_I^2 \gamma_S^2 S(S+1)}{15 \quad r_{IS}^6} X_{IS} \tag{3}$$

where

$$X_{IS} = J(\omega_I - \omega_S) + 3J(\omega_I) + 6J(\omega_I + \omega_S) \tag{4}$$

and

$$J(\omega) = \frac{2\tau_R}{1 + \omega^2 \tau_R^2} \tag{5}$$

Where $\Delta\sigma$ is an effective chemical shift anisotropy ($\sigma_{\parallel} - \sigma_{\perp}$ for an axially symmetric case), N_S is the number of chemically, and structurally identical S spins (protons, nitrogens, etc.) and τ_R is the reorientational correlation time for effective isotropic-tumbling. The other symbols are standard.

Using the approach of Kuhlmann, Grant and Harris(21) for calculating NOE values in systems having three different magnetic nuclei (^{13}C, ^{14}N and ^{1}H in this study), one may calculate the NOE for the carbon-13 isotope, under proton decoupling only, from the following

$$\eta_C = \frac{\gamma_H \gamma_C f_{CH} R_{1N} - \gamma_H \gamma_C f_{CN}^2}{\gamma_C^2 R_{1N} R_{1C} - \gamma_N \gamma_H f_{CN} f_{CH}} \tag{6}$$

where

$$f_{ij} = 6J(\omega_i + \omega_j) - J(\omega_i - \omega_j) \qquad (7)$$

and $R_{1N} = \sum_S R_{NS}$ and $R_{1C} = \sum_S R_{CS}$

as defined above. The value for η_C differ slightly from the standard expression given for the carbon-proton NOE neglecting the presence of the nitrogen spin. Thus

$$\eta_C \cong \frac{\gamma_H f_{CH}}{\gamma_C R_{1C}} \qquad (8)$$

Use of Equation 1 not only neglects the cross terms between various R_{IS} terms (the cross correlated power densities) but it also assumes a negligible cross term between the R_{CSA} and R_{IS} terms. Theoretical estimates (22) of this interference term indicates its importance in deviations from single exponential behavior, but so far an experimental verification of its importance is lacking. Furthermore, its effect on inversion recovery, proton-decoupled data should be rather small.

While the assumption of isotropic rigid body tumbling may approximate the motion for the stems and other rigid portions of the tRNA molecule, this assumption may break down seriously for segments of the molecule undergoing internal motion and for sections of the loops exposed to the aqueous protons in the water media. Attention to details of segmental motion go beyond the scope of our theoretical treatment, but experimental anomalies may suggest the importance of such terms, as noted below.

Hydrogen atoms at N_3 and C_5 were assumed to exert the primary influence in proton-carbon dipolar relaxation, and N_3 for nitrogen-carbon dipolar effects. Distances from the C_4 to these protons and N_3 were determined using bond lengths and angles from crystallographic data on uridine (23) and dihydrouridine (24). The following distances (in Å) were used: C-H (1.08); C-N (1.37); N-H (1.10); in uracil, $\overleftrightarrow{C_4\text{-}N_3\text{-}H}$ (2.03); $\overleftrightarrow{C_4\text{-}C_5\text{-}H}$ (2.16); $\overleftrightarrow{C_4\text{-}C_5\text{-}C_6\text{-}H}$ (3.40); in dihydro uracil $\overleftrightarrow{C_4\text{-}C_5} < \begin{matrix} H\ (1.96) \\ \overleftrightarrow{H}\ (2.07) \end{matrix}$. The value for $\Delta\sigma$ was taken to be 160 ppm (25) for all residues except dihydrouracil, for which we studied the

TABLE II

Predicted Spin-Lattice Relaxation Parameters and Rotational Correlation Times for Uridine C_4 Carbons in E. Coli $tRNA_1^{Val}$ at 34°C[a]

Peak (Fig. 2)	T_1^{CSA}	T_{1D}^{N}	T_{1D}^{H}	τ_R
1 (S^4U_8)	3.41	32.7	7.07	11.2
	3.74	35.9	18.3	12.3
2 (D_{17})	6.03	57.7	6.52	20.3
	5.81	55.7	9.46	19.5
3	4.13	39.6	8.02	13.7
	6.36	60.9	31.2	21.4
4	5.65	54.1	11.0	19.0
	5.94	56.9	29.2	20.0
5	5.13	49.2	9.98	17.2
	4.93	46.3	24.2	16.5
9	4.32	41.4	8.4	14.4
	4.59	46.9	24.0	16.4
11 (rT_{54})	5.42	51.9	15.0	18.2
	5.69	54.5	68.6	19.1
12	3.84	36.8	7.45	12.7
	6.46	61.9	31.7	21.8
13 (V_{34})	5.07	48.5	16.7	17.0
	9.04	86.6	360.0	30.7

(a) T_1's in seconds, τ_R in nanoseconds. Values have also been predicted at 20, 26, and 40°C: they order with the 34° data above and the experimental data in Table I. First entry, 80% H_2O; second, 100% D_2O.

effects of varying $\Delta\sigma$ in 20 ppm increments from 140 to 200 ppm.

Table II contains the calculated contributions to T_1 from the three mechanisms and the correlation times for isotropic reorientation at 34°C in 80% H_2O and in 100% D_2O solvent. Several interesting features emerge upon comparing the calculated and experimental T_1's (Table I). We estimate that the CSA contribution accounts for 60-75% of the relaxation for these quaternary carbons at 6.3 Tesla. Of the 25-40% due to dipolar effects, all but 6-8% is due to nearby protons.

The range of τ_R, 12-30 nsec, is of similar magnitude reported by others, e. g., in ^{13}C studies of bulk tRNA (20, 26), and ^{31}P-nmr (8) and pulsed fluorometry (27) of yeast $tRNA^{Phe}$.

Applicability of the model

If the model is realistic, with respect to those atoms contributing to dipolar relaxation, the τ_R's calculated at 34°C in H_2O and D_2O solvents should be similar. One can see that for "Class II" peaks #4, 5, 9 and 11 (rT_{54}), the τ_R's are indeed quite comparable (due to coalescence in D_2O, peaks 6 & 7 could not be monitored). It is reasonable to suppose that the residues giving rise to these resonances are in stems or other relatively rigid regions of the molecule.

Several resonances displayed relaxation behavior which could not be reconciled with the model. These interesting anomalies, which could provide information about regional and local dynamics, include the following:

Peaks #3, 12 and V_{34} - For Class I peaks #3 and 12 and V_{34} (Class III) the τ_R's between H_2O and D_2O differ by nearly a factor of two; the large diminuition of relaxation rate in going from H_2O to D_2O might occur if solvent is more readily accessible, for example in loop segments. Thus peaks #3 and #13 may be due to uracil located in loops, as is the case for V_{34}. The very large solvent effect for this latter unusual uracil in the wobble position may be due in part to the fact that divalent metal binds to the carboxylate (De and Schweizer, unpublished), thus one is replacing approximately six solvent molecules about the cation, in this case Mg(II).

No better agreement between H_2O and D_2O solvents was found for peaks #3 and 12 if either were considered to arise from pseudouridine (Ψ_{55}), therefore not having a proton at C_5.

S^4U_8 - It is of interest to note the considerably smaller T_1 (and τ_R) and the large dependence of R_1 on temperature (Fig. 4) for S^4U_8. This residue participates in a tertiary H-binding interaction with A_{14} (12) involving the N_3-H. Even at 40°C ^{1}H-nmr studies show this H-bond is intact. However, motion of the proton dipole may exhibit a shift in frequency distribution ("breathing rate") toward the ^{13}C Larmor value with temperature increase, providing more efficient relaxation of C_4. Thus it appears that gradual weakening of the tertiary interaction occurs from 20°-40°C.

rT_{54} - Although the R_1 vs temperature behavior exhibited by this "Class II" residue from 20°-34°C (Fig. 5) is what we expect from a rigidly constrained monomer, it is interesting to note the large rise in R_1 between 34° and 40°C. What we are observing here is undoubtedly incipient melting of the tertiary intraloop interaction involving rT_{54} and A_{58} (28).

D_{17} - Dihydrouridine (D_{17}), like V_{34}, displays very little net change in R_1

vs. temperature (class III behavior). This may indicate the presence of independent local motion. Previous results have been interpreted in terms of D-loop flexibility (20,26). From the comparisons in Table II, there is nothing to indicate anything unusual about D_{17}; no peculiar solvent effects are exhibited. Characteristics of the tertiary folding between D- and TΨCG loops (Fig. 3) may push D_{17} into the molecular interior so that solvent is inaccessible.

There was some concern about the use of 160 ppm for $\Delta\sigma$ determined for uridine (25) since we are dealing with the saturated C_5-C_6 segment in D_{17}. We studied the effect of varying $\Delta\sigma$ in 20 ppm increments from 140 to 200 ppm upon the calculated relaxation parameters (Table III). The closest match between parameters calculated for H_2O and D_2O solvents was obtained using $\Delta\sigma$ = 200 ppm. Employing the higher $\Delta\sigma$ also results in a change in estimated CSA contribution to the spin-lattice relaxation from 49 to 60%, the latter percentage equivalent to the results calculated for the various uridines (Table II).

NOE Measurements

We have measured NOE's for the various C_4 peaks as a means of detecting potential flexibility in the D-loop (Table IV). The η values for D_{17} are

TABLE III

Effect of Varying $\Delta\sigma$ on Predicted Relaxation Parameters for Dihydrouridine (D_{17}) at 34°C[a]

$\Delta\sigma$ (ppm)	T_1^{CSA}	T_{1D}^{N}	T_{1D}^{H}	τ_R
140	6.96	51.1	5.76	17.9
	6.55	48.1	8.16	16.8
160	6.03	57.7	6.52	20.3
	5.81	55.7	9.46	19.5
180	5.38	65.3	10.9	23.0
	5.30	64.3	6.78	22.6
200	4.92	73.7	8.33	26.1
	4.94	73.9	12.6	26.1

(a) T_1's in seconds, τ_R in nanoseconds. First entry is for 80% H_2O, second for 100% D_2O.

consistently higher (0.3 - 0.6) than for other uridines (0.1 to 0.3) which is to be expected for residues in more mobile segments. The larger enhancements for the D_{17} C_4 carbonyl were also observed in D_2O solvent in contrast to the observations of Hamill, et. al.(20), for the unfractionated Salmonella tRNA mixture. On the basis of these measured η's, we would say that the D_{17} undergoes local motion which is faster than the rate of overall molecular reorientation in agreement with previous studies (20, 26).

Also listed in Table III are η values calculated as per Equations 6-8 above. Since the model assumes overall isotropic molecular reorientation in a motional regime outside extreme narrowing and does not provide for segmental modulation, it is not surprising that the calculated η's are small and near 0.1, the expected limit for slowly tumbling molecules.

Although the η values for V_{34} are not significantly larger than uridines,

TABLE IV

Measured and Calculated Nuclear Overhauser Enhancements, η, for Uracil C_4 Carbonyls in E. coli $tRNA_1^{Val}$ (a)

Peak (b)	Assignment	20°		26°		34°		40°	
1	S^4U_8 (c)	-0.08	.048	0.06	.047	0.06	.048	0.24	.049
2	D_{17}	0.52	.071	0.64	.070	0.27	.070	0.44	.071
3	U	0.21	.049	0.24	.049	0.12	.049	0.07	.050
4	U	0.10	.049	0.27	.049	0.17	.049	0.25	.049
5	U	0.19	.049	0.20	.049	0.18	.049	0.22	.049
6	U	0.25		0.17		(d)		(d)	
7	U	0.19	.049	0.17	.048	0.13	.049	0.25	.049
8	(d)			(d)		(d)		(d)	
9	U	0.27	.049	0.19	.049	0.10	.049	0.24	.049
10	(d)			(d)		(d)		(d)	
11	rT_{54}	0.20	.038	0.11	.038	0.07	.038	0.01	.038
12	U	0.27	.049	0.15	.049	0.08	.050	0.01	.050
13	V_{34}	0.22	.033	0.08	.033	0.18	.033	0.27	.033

(a) Peak intensities compared between spectra taken with decoupler on continuously (+NOE) and with decoupler gated off (-NOE) during delay of $5T_1$ (20 sec) between 90° observe pulses. 2000 transients transformed; solution conditions as in Figure 3. Estimated error limits ±0.1. Calculated values in second column for each temperature.

(b) Peaks are numbered from low to high field (see Table I and Figure 3).

(c) Difficult to measure due to low intensities for S^4U

(d) Unable to measure

in contrast to those for D_{17}, three findings may be interpreted in terms of flexibility in the anticodon loop segment containing V_{34}: 1) the relatively invariant response of R_1 to temperature cited above; 2) the low R_1 itself, 0.24 - 0.27 sec^{-1} (Fig. 5); 3) the facile temperature induced destacking of V_{34} from A_{35} and other purine bases in the anticodon loop as monitored by downfield shifting (Figs. 1 & 2).

Conclusions

From these experimental and theoretical studies we can construct the following conceptualization of $tRNA_I^{Val}$ structural dynamics in solution over the physiologiclly relevant temperature range 20-40°C. The secondary and tertiary solution structure promulgated earlier (1, 6, 12) remains essentially intact over these temperatures. However, the tertiary interactions involving s^4U_8 are gradually loosened as temperature rises and there is incipient melting of the rT_{54}-A_{58} tertiary bond between 34° and 40°C.

We confirm that the loop segment containing dihydrouridine is more flexible than the overall molecular backbone. In addition, we find that the anticodon loop is indeed also quite flexible, as monitored by V_{34} in the wobble position of the anticodon.

The similar solvent effects on C_4 T_1's observed for V_{34}, #3, and #12 indicates that the latter two uridines are probably also located in loops where solvent is readily accessible and tertiary interaction is not occurring. With reference to Fig. 1, the likely candidates are U_{33}, U_{59}, U_{49} or Ψ_{55}, although the latter supposedly undergoes tertiary H-bonding with G_{18} in the D-loop (28). Those residues more rigidly held in secondary (stems) and tertiary interactions with τ_R's characteristic of the tRNA molecule itself may produce peaks #4, 5, 6, 7, and 9. Again with reference to Fig. 1, the corresponding residues may be U_4, U_7, U_{12}, U_{29}, U_{64}, or U_{67}.

Acknowledgements

This work was supported in part by USPHS grants GM25512 (MPS) AND GM-08521 (DMG). The JEOL FX-270, located in the Department of Medicinal Chemistry, was financed in part by NSF grant PCM7922984.

*Presented in part at the VII International Biophysics Congress and III Pan-American Biochemistry Congress, Mexico City, August 23-28, 1981.

[3]Correspondence should be addressed to this author.

[4]Present address: Forest Sciences Lab., U.S. Forest Service, Albuquerque, NM 87106, USA.

[5]Present address: Digital Equipment Corp., Colorado Springs, CO 80919, USA.

REFERENCES

1. Reid, B. R. and Hurd, R. E. (1977) Accounts Chem. Res. 10, 396-402.
2. Bolton, P.H. and Kearns, D. R. (1978) in Biological Magnetic Resonance, eds. Berliner, L. J. and Reuben, J., Plenum Press, New York, vol I, pp. 91-137.
3. Patel, D. J. (1978) Ann. Rev. Phys. Chem., 29, 337-362.
4. Robillard, G. T. and Reid, B. R. (1979) in Biological Applications of Magnetic Resonance, Ed. Shulman, R. G., Academic Press, New York, pp. 45-112.
5. Schimmel, P. R., Redfield, A. G. (1980) Ann. Rev. Biophys. Bioeng. 9, 181-221.
6. Reid, B. R. (1981), Ann. Rev. Biochem. 50, 969-996.
7. Salemink, P. J. M., Swarthof, T. and Hilbers, C. W. (1979) Biochemistry 10, 3477-3485.
8. Gorenstein, D. G. and Luxon, B. A. (1979) Biochemistry, 18, 3796-3804.
9. Schweizer, M. P., Hamill, Jr., W. D., Walkiw, I. J., Horton, W. J. and Grant, D. M. (1980) Nucleic Acids Research 8, 2075-2083.
10. Agris, P. F. and Schmidt, P. G. (1980) Nucleic Acids Research 8, 2085-2091.
11. Yokoyama, S., M. J. Usuki, K., Yamaizumi, Z., Nishimura, S. and Miyazawa, T. (1980) FEBS Lett., 119, 77-80.
12. Reid, B. R., McCollum. L., Ribiero, N. S., Abbate, J. and Hurd, R. E. (1979) Biochemistry 18, 3996-4005.
13. Johnston, P. D. and Redfield, A. G. (1979) in Transfer RNA: Structure, Properties and Recognition, Eds. Shimmel, P. R., Soll, D. and Abelson, J. N., Cold Spring Harbor Laboratory, pp. 191-206.
14. Sigler, P. B. (1975) Ann. Rev. Biophys. Bioeng. 4, 477-527.
15. Robertus, J. D., Ladner, J. E., Finch, J. T., Rhodes, D. Brown, R. S., Clark, B. F. C. and Klug, A. (1974) Nature 250, 546-551.
16. Kim, S. H., Sussman, J. L., Suddath, F. L., Quigley, G. J., McPherson, A., Wang, H. J.,Seeman, N. C., and Rich, A. (1974) Proc. Natl. Acad. Sci. USA 71, 4970-4974.
17. Canet, D., Levy, G. C., and Peat, I. R. (1975) J. Magn. Resonance 18, 199 204.
18. Harada, F., Kimura, F. and Nishimura, S. (1971) Biochemistry 10, 3269-3276.
19. Harada, F., Kimura, F. and Nishimura, S. (1971) ibid 10, 3277-3283.
20. Hamill, Jr., W. D., Horton, W. J., and Grant, D. M. (1980) J. Am. Chem. Soc. 102, 5454-5458.
21. Kuhlmann, K. F., Grant, D. M. and Harris, R. K., (1970), J. Chem. Phys. 52, 3439-3438.
22. Werbelow, L. G., Hamill, Jr., W. D. and Grant, D. M., Unpublished results.
23. Steward, R. F. and Jensen, L. H. (1967) Acta. Crystallogr. 23, 1102-1105.
24. Rohrer, D. C. and Sundaralingam, M. (1970) ibid B. 26, 546-553.
25. Hamill, Jr., W. D. (1977) Ph.D. Dissertation, University of Utah.
26. Komoroski, R. A. and Allerhand, A. (1972) Proc. Nat'l. Acad. Sci. USA 69, 1804-1808.
27. Ehrenberg, M., Rigler, R., and Wintermeyer, W. (1979) Biochemistry 18, 4588-4599.
28. Hurd, R. E. and Reid, B. R. (1979) Biochemistry 18, 4005-4011.